

Multi-level magnetic microrobots delivery strategy within a hierarchical vascularized organ-on-a-chip

Kangyi Lu,^a Chenyang Zhou,^a Zhangjie Li,^a Yijun Liu,^a Feifan Wang,^a Lian Xuan^b and Xiaolin Wang^{*a,b,c,d}

^a Department of Micro/Nano Electronics, School of Electronic Information and Electrical Engineering, Shanghai Jiao Tong University, Shanghai, 200240, China.

^b Institute of Medical Robotics, Shanghai Jiao Tong University, Shanghai, 200240, China.

^c National Key Laboratory of Advanced Micro and Nano Manufacture Technology, Shanghai Jiao Tong University, Shanghai, 200240, China.

^d National Center for Translational Medicine (Shanghai) SHU Branch, Shanghai University, Shanghai, 200444, China.

Corresponding author:

Xiaolin Wang

Email: xlwang83@sjtu.edu.cn; Tel: +86 (021) 3420-6683

Supplemental Movie S1: Demonstration of magnetic steering capability of the fabricated microrobotic guidewire in 3D space.

Supplemental Movie S2: Selective navigation of the microrobotic guidewire in a 2D coronary intervention simulator and a 3D vascular phantom.

Supplemental Movie S3: Superparamagnetic microrobots assemble from suspensions into swarms.

Supplemental Movie S4: Movement locus tracking of microrobot chain and swarm.

Supplemental Movie S5: Demonstration of the multi-level microrobot delivery within a two-tier branching microfluidic chip.

Supplemental Movie S6: Perfusion of fluorescent microbeads with a diameter of 5 μm inside vessel lumens.

Supplemental Movie S7: Perfusion of 70 kDa FITC-dextran inside vessel lumens without non-physiological leakage.

Supplemental Movie S8: Magnetic navigation of microrobot swarms within EC-lined microfluidic channels and capillary lumens.

Supplemental Movie S9: Homogeneous behavior of microrobot swarms and their dissolution upon the removal of actuation field.

Supplemental Figure S1:

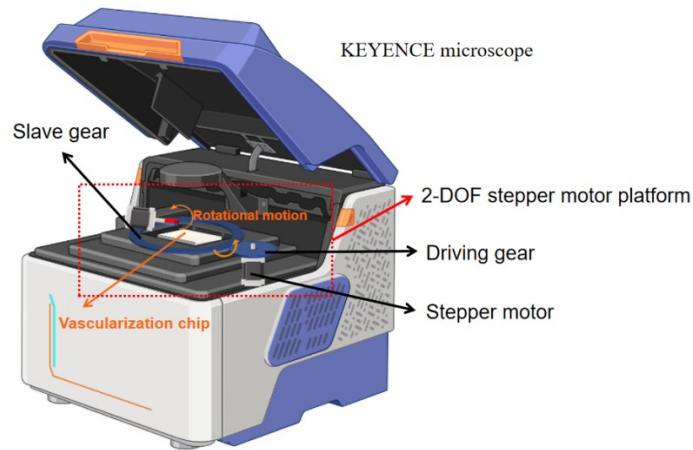


Fig. S1 Diagram of the magnetic control device setup. Magnetic navigation of the microrobotic guidewire is achieved through manipulating the position of the piezoelectric specimen stage of the KEYENCE microscope in the x - y plane. The magnetic manipulation of microrobots was achieved by controlling both the direction and frequency of the rotating magnetic field through adjusting the position of the 2-DOF motor platform relative to the chip and modulating the rotational speed of the motor, respectively.

Supplemental Figure S2:

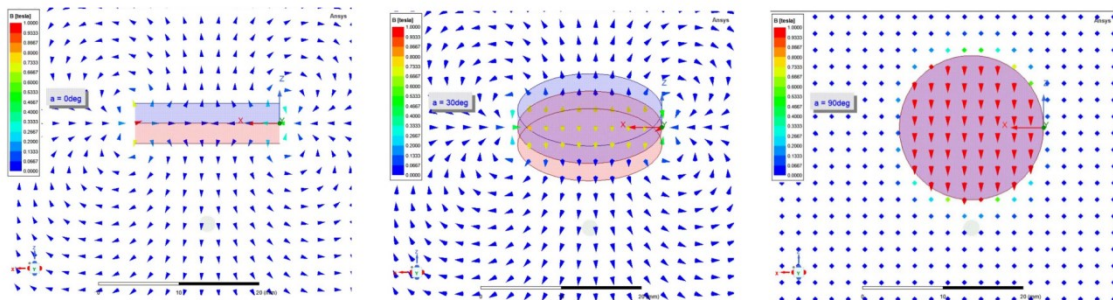


Fig. S2 Ansys simulation results of the magnetic field strength and directions within the workspace of the permanent magnet at 0°, 30°, and 90° degrees, respectively.

Supplemental Table 1: Parameters of the microrobotic guidewire used in simulation

Notation (Description)	Value	Unit
OD (Outer diameter)	700	μm
ID (Inner diameter)	160	μm
L (Length)	20	mm
E (Young's modulus)	1.367	MPa
P_{PDMS} (Poisson ratio of PDMS)	0.49	
P_{NdFeB} (Poisson ratio of NdFeB)	0.24	
M (Magnitude of magnetization)	128	kA/m

Supplemental Figure S3:

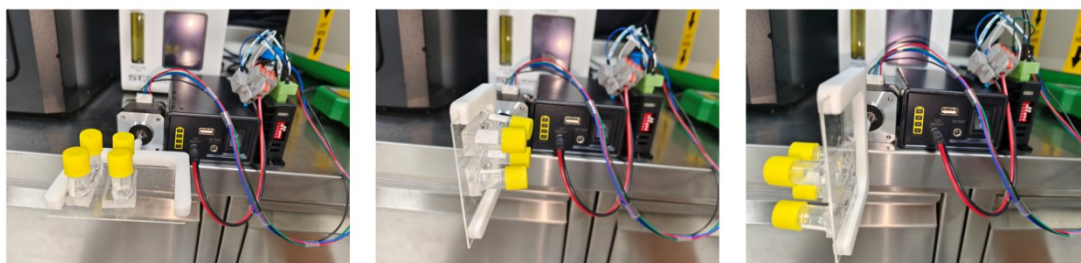


Fig. S3 A motorized rotational apparatus for EC-lining. The microfluidic device was subjected to a 90° rotation every 15 minutes for a duration of 4 hours, effectively facilitating the uniform adherence of ECs onto the channel surfaces.

Supplemental Figure S4:

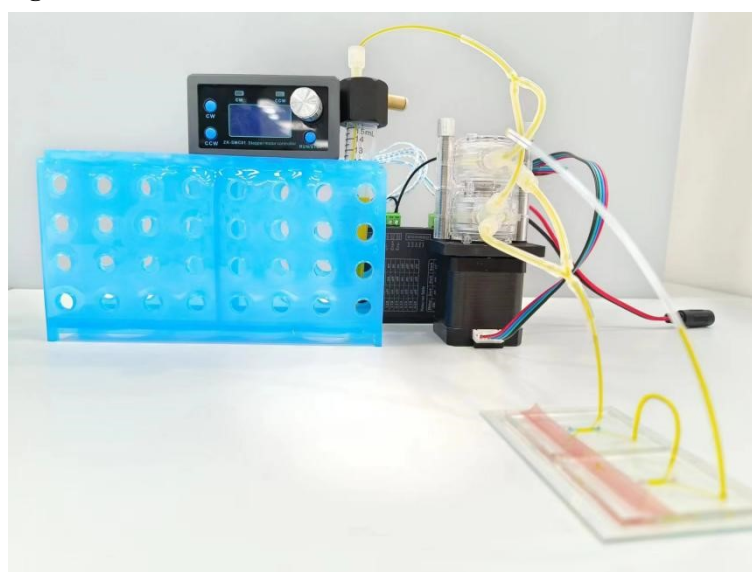


Fig. S4 The peristaltic pump device used for establishing a flow environment within a microfluidic chip.

Supplemental Figure S5:

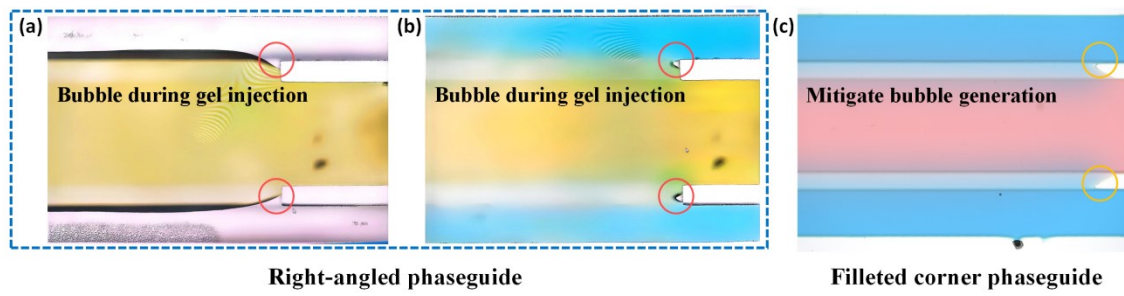


Fig. S5 Comparison of right-angled and filleted corner phaseguide design. (a)-(b) Right-angled phaseguide design: bubble formation during gel injection and media perfusion. (c) Filleted corner phaseguide design demonstrating effective reduction in bubble generation.

Supplemental Figure S6:

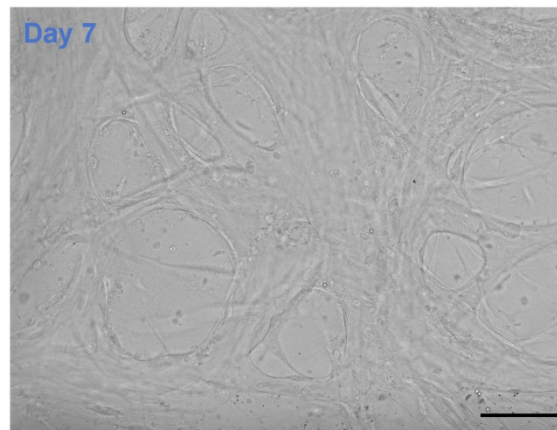


Fig. S6 High-magnification bright-field image displays blood lumens with distinct outlines. (Scale bar, 50 μm).